Available online at www.sciencedirect.com
SCIENCE DIRECT®
Biochemical and Biophysical Research Communications 313 (2004) 129–134
BBRC
www.elsevier.com/locate/ybbrc

Escherichia coli $tRNA_4^{Arg}$(UCU) induces a constrained conformation of the crucial Ω-loop of arginyl-tRNA synthetase☆

Yong-Neng Yao,[a] Qing-Shuo Zhang,[a] Xian-Zhong Yan,[b] Guang Zhu,[b] and En-Duo Wang[a,*]

[a] *State Key Laboratory of Molecular Biology, Institute of Biochemistry and Cell Biology, Shanghai Institutes for Biological Sciences, The Chinese Academy of Sciences, 320 Yue Yang Road, Shanghai 200031, PR China*

[b] *Department of Biochemistry, The Hong Kong University of Science and Technology, Clear Water Bay, Kowloon, Hong Kong SAR, PR China*

Received 22 September 2003

Abstract

Previous investigations show that $tRNA^{Arg}$-induced conformational changes of arginyl-tRNA synthetase (ArgRS) Ω-loop region (*Escherichia coli* (*E. coli*), Ala451–Ala457) may contribute to the productive conformation of the enzyme catalytic core, and *E. coli* $tRNA_2^{Arg}$(ICG)-bound and -free conformations of the Ω-loop exchange at an intermediate rate on NMR timescale. Herein, we report that *E. coli* ArgRS catalyzes $tRNA_2^{Arg}$(ICG) and $tRNA_4^{Arg}$(UCU) with similar efficiencies. However, ^{19}F NMR spectroscopy of 4-fluorotryptophan-labeled *E. coli* ArgRS reveals that the $tRNA_4^{Arg}$(UCU)-bound and -free conformations of the Ω-loop region interconvert very slowly and the lifetime of bound conformation is much longer than 0.33 ms. Therefore, $tRNA_4^{Arg}$(UCU) differs from $tRNA_2^{Arg}$(ICG) in the conformation-exchanging rate of the Ω-loop. Comparative structure model of *E. coli* ArgRS is presented to rationalize these ^{19}F NMR data. Our ^{19}F NMR and catalytic assay results suggest that the $tRNA^{Arg}$-induced conformational changes of Ω-loop little contribute to the productive conformation of ArgRS catalytic core.

Keywords: Aminoacyl-tRNA synthetase; Arginine; tRNA; argU; Comparative modeling; ArgRS

Aminoacyl-tRNA synthetases (aaRSs) are responsible for the esterification of amino acids and their cognate tRNAs, and therefore play crucial roles in protein translation in vivo [1,2]. Twenty aaRSs are cognate to 20 amino acids in all species except a few archaea [1,2]. Most of these 20 aaRSs catalyze the whole esterification reaction in two steps: (1) activation of the amino acid and (2) transfer of the activated amino acid to the 3′- or 2′-hydroxyl moiety of the tRNA-CCA termini [1,2].

Arginyl-tRNA synthetase (ArgRS, EC 6.1.1.19) is a member of the class I aaRSs, which are characterized by the 'HIGH' and 'KMSKS' structural motifs [2]. ArgRS has been investigated extensively, but its atypical catalytic mechanism remains to be elucidated [3–10]. ArgRS, like glutamyl- and glutaminyl-tRNA synthetases, requires its cognate tRNA for the activation of amino acids [3–10]. The crystal structure of yeast ArgRS bound to arginine in the catalytic core and yeast $tRNA^{Arg}$(ICG) has been characterized to a resolution of 2.2 Å [6]. Major structural changes of the anticodon-binding domain (Add-2 domain) in yeast ArgRS are observed on two peptides in the presence of $tRNA^{Arg}$ [6]. Specifically, the first peptide of yeast ArgRS goes from strand S13 to helix H15, and the second peptide is composed of strand S14, helix H17, and the Ω-loop [6]. These two structural changes in the anticodon-binding domain of yeast ArgRS may be involved in the mechanism of tRNA-required arginine activation [6].

☆ *Abbreviations: Escherichia coli*, *E. coli*; aaRSs, aminoacyl-tRNA synthetases; ArgRS, arginyl-tRNA synthetase; $tRNA_2^{Arg}$(ICG), transfer RNA isoacceptor for arginine (ICG); ^{19}F NMR, fluorine-19 nuclear magnetic resonance; 4-F-Trp, 4-fluorotryptophan; FWT, 4-F-Trp-labeled *E. coli* ArgRS; $tRNA_4^{Arg}$(UCU), transfer RNA isoacceptor for arginine (UCU); IPTG, 1-isopropyl-β-D-1-thiogalactopyranoside.

* Corresponding author. Fax: +86-21-54921011.
E-mail address: edwang@sibs.ac.cn (E.-D. Wang).

0006-291X/$ - see front matter © 2003 Elsevier Inc. All rights reserved.
doi:10.1016/j.bbrc.2003.11.107

Local conformational changes in *Escherichia coli* ArgRS induced by its substrates, specifically, arginine, ATP, and the transfer RNA isoacceptor for arginine (ICG) ($tRNA_2^{Arg}$(ICG)), were previously investigated by fluorine-19 nuclear magnetic resonance (^{19}F NMR) spectroscopy of 4-fluorotryptophan (4-F-Trp)-labeled *E. coli* ArgRS (FWT) in which five Trp residues (Trp162, -172, -228, -349, and -446) were substituted with 4-F-Trp [10]. In this earlier study, the five fluorine resonances observed in the ^{19}F NMR spectrum were assigned to the five 4-F-Trp residues of FWT. The authors reported that arginine and/or $tRNA^{Arg}$ induce distinct local conformational changes in the catalytic core of the enzyme, and the anticodon stem of $tRNA^{Arg}$ interacts with the Ω-loop of *E. coli* ArgRS [10].

The *argU* gene encodes a rare transfer RNA isoacceptor for arginine (UCU) ($tRNA_4^{Arg}$(UCU)) for the rarely used arginine codons, AGA/AGG, in *E. coli* [11,12]. However, AGA/AGG codons frequently encode the arginine residue in eukaryotes [13]. Detailed interactions between $tRNA_4^{Arg}$(UCU) and *E. coli* ArgRS have not been investigated to date. In the present study, $tRNA_4^{Arg}$(UCU) was purified from an *E. coli* overexpressing strain. Catalytic kinetic assays for $tRNA_4^{Arg}$(UCU) of *E. coli* ArgRS were compared with previously reported data for $tRNA_2^{Arg}$(ICG) [14]. ^{19}F NMR spectroscopy was performed to investigate the conformational changes in FWT induced by $tRNA_4^{Arg}$(UCU). Additionally, a comparative model of *E. coli* ArgRS, constructed using a template based on the yeast ArgRS crystal structure [6], is employed to rationalize the ^{19}F NMR data. Finally, in view of the NMR results obtained herein and the crystal structure of yeast ArgRS [6], the relationship between the two $tRNA^{Arg}$-binding sensitive peptides in the Add-2 domain of ArgRS and the productive conformation of the ArgRS catalytic core is discussed.

Materials and methods

Materials. All chemicals were purchased from Sigma (USA) unless otherwise specified. All restriction enzymes were purchased from New England Biolabs (Canada). FWT used for ^{19}F NMR was prepared in our laboratory [10]. The pSBET-b plasmid [15] harboring the *argU* gene and the expression plasmid-pBCP378 [16] were kindly donated by Dr. Gangloff, J. (IMBC, CNRS, France).

Production of $tRNA_4^{Arg}$(UCU). The *argU* gene was isolated from pSBET-b by digestion with *Hin*cII and *Sph*I. The −35 promoter region of *argU* was removed and the remaining fragment containing the region encoding $tRNA_4^{Arg}$(UCU) was recombined into the *Nde*I and *Sph*I cloning sites of pBCP378. The recessed 3′ termini of the *Nde*I site in pBCP378 were repaired by T4 DNA polymerase to facilitate ligation to the *Hin*cII blunt end of the *argU* fragment. The resulting construct was identified as pBCP378-*argU* by DNA sequencing. *E. coli* host MT102 cells (*ara*Δ139, Δ(*ara*, *leu*) 7697, Δ*lac*X74, *gal*U, *gal*K, *str*A, and *hsd*R) were transformed with pBCP378-*argU*. The $tRNA_4^{Arg}$(UCU) was over-expressed by induction with 1 mM 1-isopropyl-β-D-1-thio-galactopyranoside (IPTG) at 37 °C in LB medium. Purification of $tRNA_4^{Arg}$(UCU) was performed as described previously [14].

Catalytic kinetic assays. Native *E. coli* ArgRS employed in catalytic kinetic assays was prepared as described in a previous report [17]. Catalytic kinetic constants of *E. coli* ArgRS for $tRNA_4^{Arg}$(UCU) were determined using the method described in [17]. Briefly, $tRNA_4^{Arg}$(UCU) concentration was varied from 0.5 to 20 μM in kinetic assay, and the catalytic reaction was initiated by adding 5 nM *E. coli* ArgRS to the reaction mixtures. The accepting activity of $tRNA_4^{Arg}$(UCU) was determined as reported previously [14].

Comparative modeling of E. coli ArgRS. A 2.2 Å crystal structure of the ternary complex formed by yeast ArgRS and its cognate $tRNA^{Arg}$ in the presence of the L-arginine substrate (Protein Data Bank code 1F7U) was used as a template for comparative modeling [6]. An automated knowledge-based protein-modeling server SwissModel (v 3.5) was used for comparative modeling [18]. Procheck (v 3.4) was used for model validation [19,20] and Swiss-Pdbviewer (v 3.7) was employed for computing the energy, structural superposition, and calculation of the root mean square (RMS) deviation value between the model and templates [18]. The docking model of *E. coli* ArgRS and $tRNA^{Arg}$ was generated by superimposing the 1F7U crystal structure and the *E. coli* ArgRS model, based on coordination of their Rossmann folding, using Swiss-Pdbviewer (v 3.7), and then merging the atomic coordinates of *E. coli* ArgRS and $tRNA^{Arg}$.

^{19}F NMR measurements. ^{19}F NMR spectroscopy was performed on a Varian Unity INOVA 600 spectrometer with a fluorine resonant frequency of 564.277 MHz, using an HF [BB] probe (Nalorac). The sample preparation techniques and ^{19}F NMR parameters employed were based on a previous report [10].

Results and discussion

Production of $tRNA_4^{Arg}$(UCU)

The $tRNA_4^{Arg}$(UCU) was overproduced in *E. coli* MT102 incorporating pBCP378-*argU*, following induction with 1 mM IPTG (Fig. 1, lane 2). The arginine-accepting activity of crude tRNAs extracted from MT102 transformants was 896 pmol/A_{260} (approximately

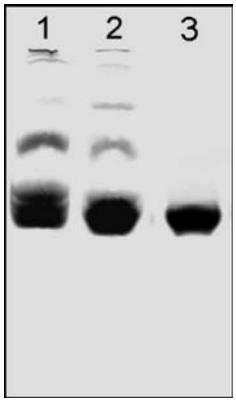

Fig. 1. Urea-PAGE analysis of $tRNA_4^{Arg}$(UCU) overexpression and purification. Total tRNAs from MT102 host cells (lane 1), crude $tRNA_4^{Arg}$(UCU) from MT102 harboring pBCP378-*argU* (lane 2), and the $tRNA_4^{Arg}$(UCU) with 90% homogeneity (lane 3) are depicted. Samples (~5 μg) were loaded and analyzed on 12% urea-PAGE. The gel was stained with toluidine blue O.

10 times that of MT102 host cells (99 pmol/A_{260})) [14]. Approximately 20 mg of $tRNA_4^{Arg}$(UCU) was isolated to 90% homogeneity from crude tRNAs above. Gel electrophoresis in the presence of urea (urea-PAGE) of $tRNA_4^{Arg}$(UCU) is depicted in Fig. 1, lane 3. The quantity and purity of $tRNA_4^{Arg}$(UCU) obtained was sufficient for use in catalytic kinetic assays and ^{19}F NMR titration.

Catalytic kinetic constants for $tRNA_4^{Arg}$(UCU)

The catalytic kinetic constants of *E. coli* ArgRS for $tRNA_4^{Arg}$(UCU) are listed in Table 1. The k_{cat} and K_m values for $tRNA_4^{Arg}$(UCU) are smaller than those for $tRNA_2^{Arg}$(ICG), indicating that $tRNA_4^{Arg}$(UCU) binds *E. coli* ArgRS more tightly than $tRNA_2^{Arg}$(ICG), and that the aminoacylation rate of $tRNA_4^{Arg}$(UCU) by ArgRS is slightly lower than that of $tRNA_2^{Arg}$(ICG). However, similar k_{cat}/K_m values were obtained for these two $tRNA^{Arg}$ isoacceptors, implying that *E. coli* ArgRS has similar catalytic specificity and efficiency for them.

Comparative model of E. coli ArgRS

To distinguish the interactions between *E. coli* ArgRS and $tRNA_4^{Arg}$(UCU) observed in ^{19}F NMR titration spectra, a comparative model for *E. coli* ArgRS was constructed based on the template (yeast ArgRS) bound to its cognate $tRNA^{Arg}$ and L-arginine [6]. The overall structure of *E. coli* ArgRS is depicted in Fig. 2A. The total energy of the *E. coli* ArgRS model is -1.57×10^4 kJ/mol, and the RMS deviation value between the model and the template (yeast ArgRS) is 0.27 Å for 537 Cα atoms, as determined by Swiss-Pdb-viewer. This low RMS deviation value indicates significant similarities between the *E. coli* ArgRS model and the crystal structure of yeast ArgRS. Procheck additionally revealed that 87.4% and 11.8% of non-Gly and non-Pro residues of the *E. coli* ArgRS model lie in favored and allowed regions of Ramachandran-plot statistics, respectively, with only 0.8% in the disallowed region. All 39 Gly residues were present in favored and allowed regions, and only one Pro residue was in a disallowed region. The results indicate good stereochemical quality of the comparative *E. coli* ArgRS model.

The five Trp residues are located in interesting regions of the *E. coli* ArgRS model. Specifically, Trp162 and Trp228 are present at the edge of the first half of the

Table 1
Kinetic constants of *E. coli* ArgRS for $tRNA^{Arg}$

	K_m (μM)	k_{cat} (s^{-1})	k_{cat}/K_m ($s^{-1}\,\mu M^{-1}$)
$tRNA_4^{Arg}$(UCU)	1.9	21.9	11.5
$tRNA_2^{Arg}$(ICG)[a]	2.5	26.0	10.4

[a] Data in this row are from [14] and an experimental control.

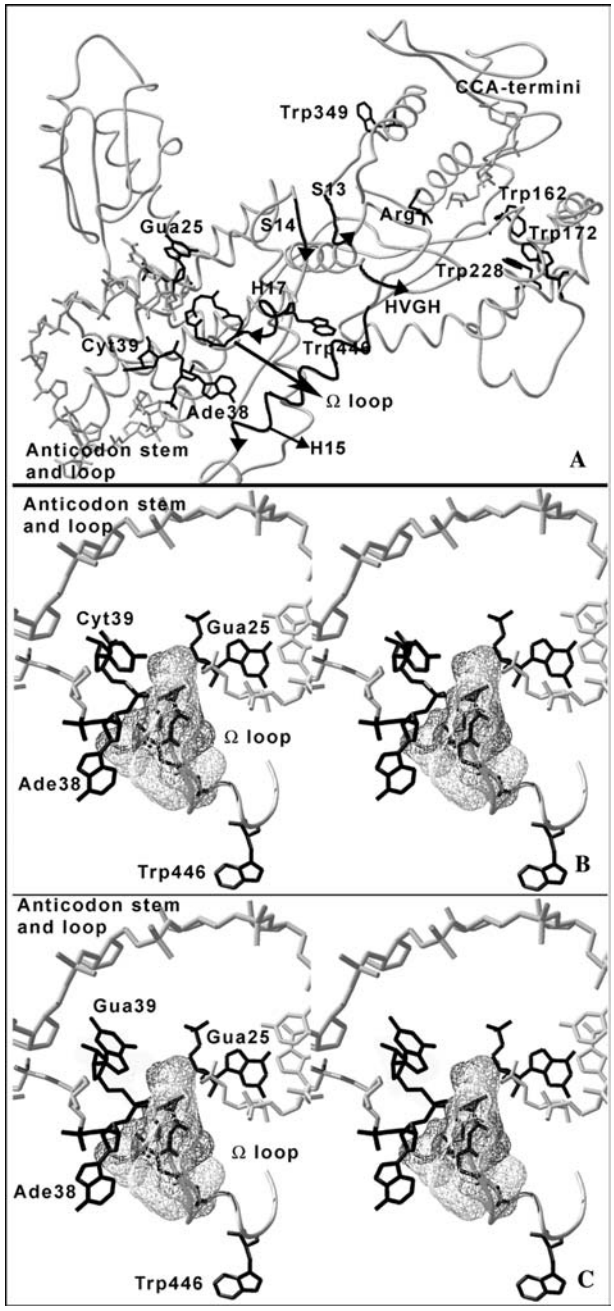

Fig. 2. The structural model of *E. coli* ArgRS. (A) The overall view of *E. coli* ArgRS bound to an L-arginine molecule in the catalytic core and partial $tRNA_2^{Arg}$(ICG). The five Trp residues are highlighted. $tRNA^{Arg}$ is partially depicted with the phosphate-ribose backbone of its CCA termini and anticodon stem and loop. Gua25, Cyt39, and Ade38 of $tRNA_2^{Arg}$(ICG) are shown with their base moieties. The $tRNA^{Arg}$-sensitive elements involving S13, H15, S14, H17, and Ω-loop are highlighted, and only the Ω-loop is illustrated with the α-carbon backbone. The "HIGH" motif of class I aaRS ("HVGH" in *E. coli* ArgRS) in the catalytic core is also indicated. (B) A detailed stereo view of the interactions between Gua25, Cyt39, and Ade38 of $tRNA_2^{Arg}$(ICG) and the Ω-loop. The molecular surface of the Ω-loop is shown. The side-chain indole ring of Trp446 is highlighted. (C) A detailed stereo view of the interactions between Gua25, Gua39, and Ade38 of $tRNA_4^{Arg}$(UCU) and the Ω-loop. The Ω-loop and Trp446 are depicted as for (B).

catalytic core (encompassing Gln113–Thr164 and Trp228–Val255), Trp349 lies in the second half of the catalytic core (Tyr311–Thr382), Trp172 is tightly buried within the Ins-1 domain (Gln165–Met227) of ArgRS, and Trp446 is located in the Add-2 domain (anticodon-binding domain, Arg383–Met577) of ArgRS, as shown in Fig. 2. Data from studies on yeast ArgRS reveal that Trp446 is part of helix H17 (Trp446–Leu450) followed by the Ω-loop (Ala451–Ala457), which is crucial for the positioning of the $tRNA^{Arg}$ anticodon stem [6]. Additionally, it is proposed that the structural changes induced by $tRNA^{Arg}$ in the local region of the Ω-loop are involved in the mechanism of $tRNA^{Arg}$-required arginine activation in ArgRS [6].

Effects of $tRNA_4^{Arg}$(UCU) on the conformation of E. coli ArgRS

The five fluorine resonances in the ^{19}F NMR spectrum of FWT were previously assigned to five 4-F-Trp residues [10], as indicated in Fig. 3A. The effects of $tRNA_2^{Arg}$(ICG) on the ^{19}F NMR spectrum of FWT were described in the earlier report (see also Figs. 3B and C).

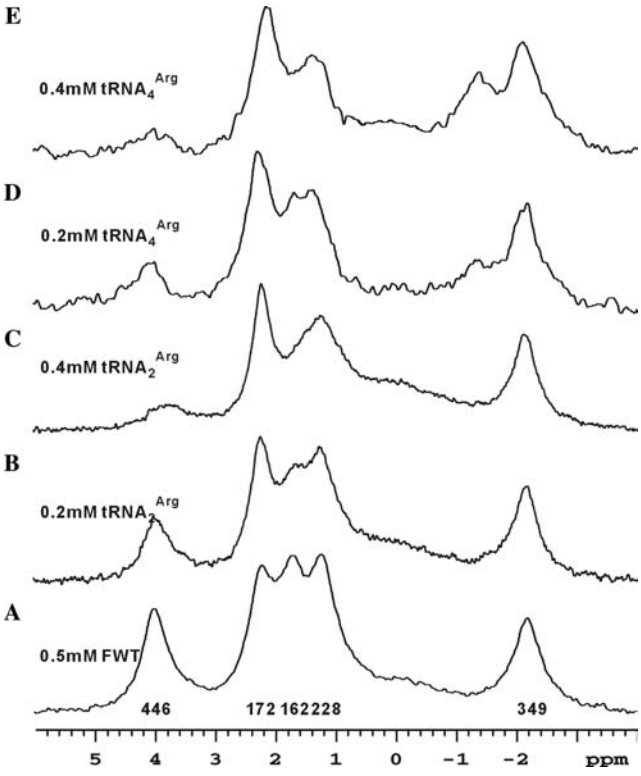

Fig. 3. Effects of $tRNA^{Arg}$ binding on the ^{19}F NMR spectra of FWT. Spectra of FWT (0.5 mM) titrated with the two $tRNA^{Arg}$ isoacceptors, $tRNA_2^{Arg}$(ICG), and $tRNA_4^{Arg}$(UCU), are presented. Substrates and their concentrations are indicated. In addition to $tRNA^{Arg}$, NMR samples contained 5% (v/v) D_2O, 0.5 mM FWT and NMR sample buffer (50 mM Tris–HCl, pH 7.5, 80 mM KCl, 8 mM $MgCl_2$, 0.1 mM EDTA, and 0.5 mM DTT). (A–C) are obtained from [10].

$tRNA_2^{Arg}$(ICG) induces distinct conformational changes in both the catalytic core in the vicinity of Trp162 and Trp228, and the local structure of the Trp446 residue [10].

The effects of $tRNA_4^{Arg}$(UCU) on the ^{19}F NMR spectrum of FWT are depicted in Figs. 3D and E. Due to the $tRNA_4^{Arg}$(UCU) binding, significant conformational changes were observed in the catalytic core near Trp162 and Trp228, similar to those described above, suggesting that $tRNA_4^{Arg}$(UCU) has a similar effect on the ArgRS catalytic core as $tRNA_2^{Arg}$(ICG). The similar effects on the catalytic core may be caused by the common CCA termini of two $tRNA^{Arg}$ isoacceptors interacting with the catalytic core of ArgRS.

An evident difference was observed between the ^{19}F NMR spectra in the presence of $tRNA_4^{Arg}$(UCU) and $tRNA_2^{Arg}$(ICG) (Figs. 3C and E). $tRNA_2^{Arg}$(ICG) induced the fluorine resonance of 4-F-Trp446 into baseline, signifying that the local structure of Trp446 was in an intermediate exchange conformation [10]. In contrast, the fluorine resonance of 4-F-Trp446 was shifted from 4.02 to −1.38 ppm, following binding of $tRNA_4^{Arg}$(UCU). Additionally, two distinct fluorine resonances of 4-F-Trp446 appeared simultaneously in the ^{19}F NMR spectrum at a molar ratio of 2:5 [$tRNA_4^{Arg}$(UCU) to FWT] (Fig. 3D). This finding indicates a constrained conformation of Trp446 in the presence of $tRNA_4^{Arg}$(UCU), which slowly exchanges with the tRNA-free conformation in ArgRS on NMR timescale. These two conformations interconvert over time at a much smaller frequency than the ^{19}F NMR frequency difference for the two conformations ($(1.38 + 4.02)$ ppm × 564.277 MHz, 3.05 kHz). In view of these findings, we propose that the lifetime of the $tRNA_4^{Arg}$(UCU)-bound state is significantly longer than 0.33 ms (1/(3.05 kHz)). In addition, one complete catalytic process for $tRNA_4^{Arg}$(UCU) occurs in 45.7 ms, as calculated from the $1/k_{cat}$ value of $tRNA_4^{Arg}$(UCU) ($21.9\ s^{-1}$). Therefore, the lifetime of the $tRNA_4^{Arg}$(UCU)-bound state is between 0.33 and 45.7 ms. Since $tRNA_2^{Arg}$(ICG) induced an intermediate exchange conformation of Trp446, the lifetime of the $tRNA_2^{Arg}$(ICG)-bound state is much shorter than that of the $tRNA_4^{Arg}$(UCU)-bound state according to the NMR timescale principle [21].

The two different $tRNA^{Arg}$ isoacceptor-bound states of the Trp446 environment may be interpreted in terms of the proposed *E. coli* ArgRS model (Fig. 2). As observed from yeast ArgRS, the Ω-loop in proximity to Trp446 is limited by Gua25 and Cyt39 of yeast $tRNA^{Arg}$, and participates in the formation of a binding pocket for Ade38 [6], which is additionally observed in a model of the *E. coli* ArgRS–$tRNA_2^{Arg}$(ICG) complex (Fig. 2A and B). However, in the *E. coli* ArgRS–$tRNA_4^{Arg}$(UCU) complex model, Cyt39 is replaced by Gua39, which may further limit the conformational

flexibility of the Ω-loop. The $tRNA_4^{Arg}$(UCU)-induced slow exchange conformation of the local structure of 4-F-Trp446 and the Ω-loop may result from steric hindrance induced by the presence of a larger nucleotide at position 39 of $tRNA^{Arg}$.

The longer lifetime of the $tRNA_4^{Arg}$(UCU)-bound state of Trp446 may lead to ArgRS having a slower aminoacylation rate for $tRNA_4^{Arg}$(UCU) than $tRNA_2^{Arg}$(ICG). However, the similar k_{cat}/K_m values of $tRNA_2^{Arg}$(ICG) and $tRNA_4^{Arg}$(UCU) (Table 1) indicate comparable specificity and efficiency of ArgRS for the two $tRNA^{Arg}$ isoacceptors. This similarity may result from compensatory interactions between other regions of $tRNA^{Arg}$ and ArgRS (i.e., in addition to the Ω-loop region), which are not detected in the ^{19}F NMR spectra of the five 4-F-Trp residues. Such compensatory interactions are possible, since the identity elements of $tRNA^{Arg}$ consist of Ade/Gua73, Cyt35, Ura/Gua36, and Ade20. In addition to the anticodon stem, the D loop and acceptor stem of $tRNA^{Arg}$ interact with ArgRS [6,7,22].

The Ω-loop peptide region little relating to the productive conformation of the catalytic core

In this report, we describe conformational changes of *E. coli* ArgRS induced by the rare $tRNA^{Arg}$ isoacceptor, $tRNA_4^{Arg}$(UCU). A comparison of ArgRS ^{19}F NMR titration spectra with $tRNA_4^{Arg}$(UCU) and $tRNA_2^{Arg}$ (ICG) (Fig. 2) indicated two different $tRNA^{Arg}$ isoacceptor-bound states of the local structure near the crucial Ω-loop. The previous ArgRS crystal structure indicates that tRNA-induced structural changes in two peptides in the anticodon-binding domain (Add-2 domain) of ArgRS may contribute to an active conformation for the catalytic core of ArgRS [6]. The first peptide (*E. coli* Met371–Ala406) goes from strand S13 to helix H15, and the second peptide (*E. coli* Tyr442–Ala457) involves strand S14, helix H17 (including *E. coli* Trp446), and the Ω-loop (*E. coli* Ala451–Ala457) (Fig. 2A) [6].

Here, we show that two $tRNA^{Arg}$ isoacceptors-$tRNA_4^{Arg}$(UCU) and $tRNA_2^{Arg}$(ICG) induce two significantly different conformations of one of the two peptides above (*E. coli* Tyr442–Ala457; including S14, H17, and Ω-loop). However, these two $tRNA^{Arg}$ isoacceptors induce similar conformations in the ArgRS catalytic core, as is evident from ^{19}F NMR signals of 4-F-Trp162 and 4-F-Trp228 residues (Fig. 3), and display comparable catalytic efficiencies in the kinetic assays (Table 1). Since such a distinct difference between the two conformational changes induced by the two $tRNA^{Arg}$ isoacceptors binding on the peptide (*E. coli* Tyr442–Ala457; S14, H17, and Ω-loop) can cause no difference to the catalytic core conformation and catalyzing efficiencies of ArgRS, $tRNA^{Arg}$-induced conformational changes of this peptide may be of little significance to the productive conformation of the catalytic core.

The other peptide (*E. coli* Met371–Ala406; S13 to H15) in the Add-2 domain is also sensitive to $tRNA^{Arg}$ binding [6]. This peptide selectively interacts with specific bases of $tRNA^{Arg}$ [6]. Therefore, the conformational changes induced by $tRNA^{Arg}$ binding to this peptide may play a major role in inducing a productive conformation of the ArgRS catalytic core. This is a reasonable assumption, in view of the finding that the peptide region (*E. coli* Gly374–Lys389) interconnecting S13 and H15 is spatially very close to the catalysis-related signature 'HVGH' motif in the *E. coli* ArgRS catalytic core. Furthermore, the conformational changes in H15 induced by $tRNA^{Arg}$ were observed to lead to some structural modifications of the 'HVGH' motif region in yeast ArgRS [6].

Acknowledgments

This work was funded by the Chinese Academy of Sciences (Grant KSCX2-2-04), Shanghai Committee of Science and Technology (Grant 02DJ140567), and Chinese Natural Sciences Foundation (Grants 30330180 and 30270310).

References

[1] M. Ibba, D. Söll, Aminoacyl-tRNA synthesis, Annu. Rev. Biochem. 69 (2000) 617–650.
[2] G. Eriani, M. Delarue, O. Poch, J. Gangloff, D. Moras, Partition of tRNA synthetases into two classes based on mutually exclusive sets of sequence motifs, Nature 347 (1990) 203–206.
[3] S.X. Lin, J.P. Shi, X.D. Cheng, Y.L. Wang, Arginyl-tRNA synthetase from *Escherichia coli*, purification by affinity chromatography, properties, and steady-state kinetics, Biochemistry 27 (1988) 6343–6348.
[4] J. Cavarelli, B. Delagoutte, G. Eriani, J. Gangloff, D. Moras, L-Arginine recognition by yeast arginyl-tRNA synthetase, EMBO J. 17 (1998) 5438–5448.
[5] M. Lazard, P. Kerjan, F. Agou, M. Mirande, The tRNA-dependent activation of arginine by arginyl-tRNA synthetase requires inter-domain communication, J. Mol. Biol. 302 (2000) 991–1004.
[6] B. Delagoutte, D. Moras, J. Cavarelli, tRNA aminoacylation by arginyl-tRNA synthetase: induced conformations during substrates binding, EMBO J. 19 (2000) 5599–5610.
[7] A. Shimada, O. Nureki, M. Goto, S. Takahashi, S. Yokoyama, Structural and mutational studies of the recognition of the arginine tRNA-specific major identity element, A20, by arginyl-tRNA synthetase, Proc. Natl. Acad. Sci. USA 98 (2001) 13537–13542.
[8] G. Eriani, G. Dirheimer, J. Gangloff, Isolation and characterization of the gene coding for *Escherichia coli* arginyl-tRNA synthetase, Nucleic Acids Res. 17 (1989) 5725–5736.
[9] M. Zhou, E.D. Wang, R.L. Campbell, Y.L. Wang, S.X. Lin, Crystallization and preliminary X-ray diffraction analysis of arginyl-tRNA synthetase from *Escherichia coli*, Protein Sci. 6 (1997) 2636–2638.
[10] Y.N. Yao, Q.S. Zhang, X.Z. Yan, G. Zhu, E.D. Wang, Substrate-induced conformational changes in *Escherichia coli* arginyl-tRNA

synthetase observed by ^{19}F NMR spectroscopy, FEBS Lett. 547 (2003) 197–200.
[11] Y. Komine, T. Adachi, H. Inokuchi, H. Ozeki, Genomic organization and physical mapping of the transfer RNA genes in *Escherichia coli* K12, J. Mol. Biol. 212 (1990) 579–598.
[12] G.M. Garcia, P.K. Mar, D.A. Mullin, J.R. Walker, N.E. Prather, The *E. coli* dnaY gene encodes an arginine transfer RNA, Cell 45 (1986) 453–459.
[13] T.L. Calderone, R.D. Stevens, T.G. Oas, High-level misincorporation of lysine for arginine at AGA codons in a fusion protein expressed in *Escherichia coli*, J. Mol. Biol. 262 (1996) 407–412.
[14] J.F. Wu, E.D. Wang, Y.L. Wang, G. Eriani, J. Gangloff, Gene cloning, overproduction and purification of *Escherichia coli* $tRNA_2^{Arg}$, Acta. Biochem. Biophys. Sinica 31 (1999) 226–232.
[15] P.M. Schenk, S. Baumann, R. Mattes, H.H. Steinbiss, Improved high-level expression system for eukaryotic genes in *Escherichia coli* using T7 RNA polymerase and rare ArgtRNAs, Biotechniques 19 (1995) 196–200.
[16] J.S. Velterop, M.A. Dijkhuizen, R. van 't Hof, P.W. Postma, A versatile vector for controlled expression of genes in *Escherichia coli* and *Salmonella typhimurium*, Gene 153 (1995) 63–65.
[17] M. Liu, Y. Huang, J. Wu, E. Wang, Y. Wang, Effect of cysteine residues on the activity of arginyl-tRNA synthetase from *Escherichia coli*, Biochemistry 38 (1999) 11006–11011.
[18] N. Guex, M.C. Peitsch, SWISS-MODEL and the Swiss-PdbViewer: an environment for comparative protein modeling, Electrophoresis 18 (1997) 2714–2723.
[19] R.A. Laskowski, M.W. MacArthur, D.S. Moss, J.M. Thornton, SFCHECK: a unified set of procedures for evaluating the quality of macromolecular structure-factor data and their agreement with the atomic model, J. Appl. Cryst. 26 (1993) 283–291.
[20] A.L. Morris, M.W. MacArthur, E.G. Hutchinson, J.M. Thornton, Stereochemical quality of protein structure coordinates, Proteins 12 (1992) 345–364.
[21] M.A. Danielson, J.J. Falke, Use of ^{19}F NMR to probe protein structure and conformational changes, Annu. Rev. Biophys. Biomol. Struct. 25 (1996) 163–195.
[22] R. Giegé, M. Sissler, C. Florentz, Universal rules and idiosyncratic features in tRNA identity, Nucleic Acids Res. 26 (1998) 5017–5035.